G3, 2025, **15(10)**, jkaf186
https://doi.org/10.1093/g3journal/jkaf186
Advance Access Publication Date: 19 August 2025
Genome Report

Genomic insights into the virulence repertoire and hemibiotrophic lifestyle of the grapevine black rot pathogen *Phyllosticta ampelicida*

Monica Colombo,[1,†] Paola Bettinelli,[2,†] Jadran Garcia ,[3,†] Giuliana Maddalena,[4] Silvia Laura Toffolatti,[4] Ludger Hausmann ,[5] Silvia Vezzulli,[2] Simona Masiero ,[6,*] Dario Cantù [3,7,*]

[1]Council for Agricultural Research and Economics, Research Centre for Genomics and Bioinformatics, Fiorenzuola d'Arda, San Protaso, PC 29017, Italy
[2]Grapevine Physiology and Breeding Unit, Research and Innovation Centre, Fondazione Edmund Mach, San Michele all'Adige, TN 38098, Italy
[3]Department of Viticulture and Enology, University of California, Davis, Davis, CA 95616, United States
[4]Dipartimento di Scienze Agrarie e Ambientali, Università degli Studi di Milano, Milano, MI 20133, Italy
[5]Julius Kühn Institute, Institute for Grapevine Breeding Geilweilerhof, Siebeldingen, RP 76833, Germany
[6]Dipartimento di Bioscienze, Università degli Studi di Milano, Milano, MI 20133, Italy
[7]Genome Center, University of California, Davis, Davis, CA 95616, United States

*Corresponding authors: Simona Masiero, Dipartimento di Bioscienze, Università degli Studi di Milano, via Celoria 26, Milano, MI 20133, Italy. Email: simona.masiero@unimi.it; Dario Cantù, Department of Viticulture and Enology, University of California, Davis, One Shields Ave, Davis, CA 95616, United States. Email: dacantu@ucdavis.edu
†These authors equally contributed to the work.

Phyllosticta ampelicida, the causal agent of grapevine black rot, is a globally emerging pathogen that infects all grapevine green tissues, with young shoots and berries being particularly susceptible. Severe infections can result in total crop loss. To investigate its virulence repertoire, we generated a high-quality genome assembly of strain GW18.1 using long-read sequencing, resulting in 22 scaffolds, including 4 complete chromosomes and 12 chromosome arms, with a total genome size of 35.6 Mb and 10,289 predicted protein-coding genes. Two additional strains (TN2 and LB22.1) were sequenced with short reads to assess intraspecies diversity. Comparative genomics revealed a conserved virulence factor repertoire, including 314 carbohydrate-active enzymes (CAZymes), 17 cytochrome P450s, 35 peroxidases, and 20 secondary metabolite biosynthetic gene clusters. Trophic lifestyle prediction based on gene content supports a biotrophic-like lifestyle consistent with hemibiotrophic pathogens. Broader comparisons with other *Phyllosticta* species and 10 plant-pathogenic fungi pointed to species-specific features, while analysis of gene family evolution identified expansions and contractions in transporters and CAZymes. These genomic resources will support efforts to better understand and manage grapevine black rot.

Keywords: fungal pathogen virulence factors; pathogenomics; cell wall degrading enzymes; secondary metabolism; effectors; *Guignardia bidwellii*; *Vitis vinifera*

Introduction

Plant diseases cause 10% to 15% of global crop losses annually, amounting to hundreds of billions of dollars (Chatterjee et al. 2016). Fungi, responsible for 70% to 80% of these diseases, are a major threat to sustainable agriculture (Marín-Menguiano et al. 2019; Stukenbrock and Gurr 2023). Grapevines depend heavily on fungicides, accounting for over 65% of all agricultural fungicide use, a figure expected to rise (Nagesh et al. 2023). Black rot, a key disease in temperate-humid regions along with downy and powdery mildew, originated in North America and was introduced to Europe in 1885 (Pirrello et al. 2019). It spreads rapidly due to the susceptibility of European grapevines and is now found worldwide, likely due to the movement of infected plant material (Pirrello et al. 2019).

Grapevine black rot is caused by the fungus *Phyllosticta ampelicida* [Engleman] Van der Aa (syn. *Guignardia bidwellii* [Ellis] Viala and Ravaz), a member of the class Dothideomycetes, order Botryosphaeriales, family Botryosphaeriaceae, and genus *Guignardia* (Fig. 1a). The pathogen infects all green grapevine organs and causes significant damage. *P. ampelicida* is classified as a hemibiotrophic ascomycete, characterized by an initial biotrophic, asymptomatic phase followed by a necrotrophic phase associated with visible symptoms and tissue damage. On leaves, infection presents as circular lesions that become brown with dark-reddish borders; pycnidia (asexual fruiting bodies) appear within the central necrotic area (Fig. 1b). On young shoots, the pathogen produces dark, elongated spots on the first internode, which may expand, girdle the shoot, and penetrate the tissue, leading to cracking or canker formation. Black pycnidia are also commonly observed at the center of these lesions. The most characteristic symptoms occur on berries, from fruit set to late veraison, beginning as small, light-brown spots that expand across the fruit surface (Fig. 1c). Infected berries soften, become spongy, then dry out into blackish-blue mummies, often bearing visible pycnidia (Kuo and Hoch 1996b). *P. ampelicida* can cause severe yield losses when environmental conditions are favorable, particularly during humid springs and summers with temperatures around 25 °C.

Received on 07 May 2025; accepted on 05 August 2025

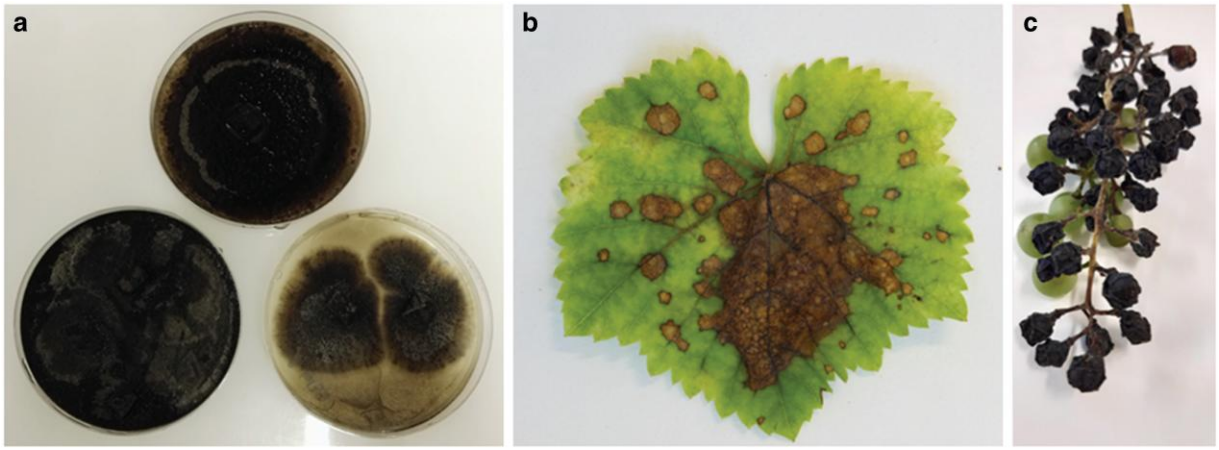

Fig. 1. Grapevine black rot. a) Axenic culture of the causal agent *P. ampelicida* (top TN2, bottom left GW18.1, bottom right LB22.1). Disease symptoms on grapevine b) leaves and c) fruits. Photos by Paola Bettinelli.

Even low disease severity can significantly impact production due to the nonlinear relationship between disease intensity and yield loss (Molitor and Beyer 2014).

The rising incidence of black rot is linked to reduced fungicide use due to the adoption of disease-resistant grapevine varieties and increased mechanical harvesting and pruning, which fail to remove infected plant material (Ullrich et al. 2009; Molitor and Beyer 2014; Hausmann et al. 2017). Mummified grape bunches often remain on vines over winter, releasing ascospores, sexual spores, in spring to initiate primary infections, while pycnidiospores spread the disease during the growing season, with both spore types germinating similarly (Ullrich et al. 2009). In Europe, the black rot surge also coincides with the ban of sterol biosynthesis inhibitors. Additionally, abandoned and uncultivated vineyards in Central Europe exacerbate the problem by acting as reservoirs, with infectious material easily spread by wind to nearby cultivated areas (Szabó et al. 2023).

To address the rise of plant pathogen resistance and reduce reliance on pesticides, alternative disease management strategies are needed. The identification of genetic resistance loci and associated molecular markers has enabled marker-assisted breeding and gene stacking in grapevine improvement programs (Vezzulli et al. 2019). More recently, genome-guided studies have begun to identify the causal genes underlying resistance quantitative trait loci (QTL), opening new opportunities for targeted genome editing (Cantu et al. 2024). In parallel, the analysis of plant pathogen genomes is critical for understanding disease emergence and spread, supporting the development of advanced diagnostics and effective curative or preventive measures (Paineau et al. 2025). New plant protection products that target essential pathogen proteins and the molecular networks activated during early infection stages are also promising (Colombo et al. 2020; Rosa et al. 2023).

A deeper understanding of pathogen virulence mechanisms is essential to guide these efforts (Paineau et al. 2025). Fungal virulence factors, such as carbohydrate-active enzymes (CAZymes), cytochrome P450s, peroxidases, transporters, secondary metabolites, and effectors play central roles in host colonization and symptom development. These factors support key processes such as cell wall penetration, nutrient acquisition, suppression of host defenses, and induction of tissue necrosis (Horbach et al. 2011; Li et al. 2025). For example, pathogens breach plant cell walls through mechanical pressure and cell wall—degrading enzymes (Pryce-Jones et al. 1999), and counteract oxidative stress via reactive oxygen species (ROS)—scavenging mechanisms such as peroxidases (Mir et al. 2015). Fungal secondary metabolites released during early infection may weaken plant defenses without triggering cell death, promoting pathogen success during the biotrophic phase (van Doorn et al. 2011; Reveglia et al. 2022).

Building on the recent release of a draft genome for *P. ampelicida* based on short-read sequencing (Eichmeier et al. 2022), we conducted further genome sequencing using long-read sequencing of a strain isolated in Germany. Additionally, to begin exploring the genetic variation within the species, we sequenced 2 strains isolated in northern Italy using short-read sequencing. To provide a broader perspective on the *P. ampelicida* virulence repertoire, comparative genomic analyses were performed within the *Phyllosticta* genus and across grapevine-pathogenic ascomycetes.

Material and methods

Isolation of *P. ampelicida* gDNA for Single Molecule Real-time sequencing Technology and short-read sequencing

A strain of *P. ampelicida* isolated by Fondazione Edmund Mach (FEM, San Michele all'Adige, Italy) in Trentino (Italy) (TN2), and one isolated by the Julius Kuhn Institute–Institute for Grapevine Breeding Geilweilerhof (Siebeldingen, Germany) (GW18.1), were previously genetically characterized (Bettinelli et al. 2023b) (Fig. 1). These fungal cultures were maintained at 24 °C on organic oatmeal agar medium (0.5% w/v) (Bettinelli et al. 2023b). The *P. ampelicida* strain LB22.1 was isolated from infected leaves during the 2022 growing season in Traona, Sondrio Province, Lombardy (Italy) and maintained on potato dextrose agar plates at 22 °C. All isolates were confirmed as *P. ampelicida* by internal transcribed spacer (ITS) analysis using primers ITS4 (TCCTCCGCTTATTGATATGC) and ITS5 (GGAAGTAAAAGTCGTAACAAGG) (Rinaldi et al. 2017). ITS sequences are available at NCBI under accession numbers PV931803, PV931804, and PV931805. High molecular weight genomic DNA (gDNA) of *P. ampelicida* isolates was extracted following the protocol of Morales-Cruz et al. (2020) with minor modifications. Specifically, we used 5 g of *P. ampelicida* mycelium and on day 2, the DNA pellet was obtained by centrifugation at 10,000 × *g* for 1 h. The quality of the extracted gDNA was assessed using a NanoDrop UV/Vis spectrophotometer and 0.8% (w/v) agarose gel. The gDNA was quantified with a Qubit 3.0 fluorometer using a Qubit dsDNA BR Assay Kit (Thermo Fisher Scientific, United States).

Library preparation and genome sequencing

The genome of *P. ampelicida* GW18.1 strain was subjected to PacBio CLR Single Molecule Real-time sequencing Technology (SMRT) to obtain high-quality long reads genomic data. To ensure optimal sequencing results, gDNA was first cleaned using 0.45× AMPure PB beads (Pacific Biosciences, Menlo Park, CA, United States) prior to library preparation. The SMRTbell template was then prepared using the SMRTbell Express Template Preparation kit 2.0 (Pacific Biosciences), following the manufacturer's instructions, with 12 µg of sheared DNA. The SMRTbell template was size-selected with a cutoff size of 17 to 80 kbp using the Blue Pippin instrument (Sage Science, Beverly, MA, United States), and the resulting size-selected library was cleaned using 1× AMPure PB beads. Finally, the library was sequenced on an SMRT cell using the PacBio Sequel II platform at the DNA Technology Core Facility of the University of California, Davis. Short-read library preparation and sequencing were performed by Novogene (Beijing, China). Libraries were prepared using the NEBNext Ultra DNA Library Prep Kit and paired-end sequencing (2×150 bp) was performed on an Illumina NovaSeq 6000 platform.

Genome assembly and scaffolding

PacBio sequencing reads for *P. ampelicida* were assembled using Falcon assembler (v.2017.06.28-18.01; Chin et al. 2016). To minimize fragmentation, we tested several length_cutoff_pr values (3 to 38 kb); a cutoff of 7 kb yielded the best assembly and was selected for final processing. Repetitive content identification in both raw and error-corrected reads was employed, as described in Minio et al. (2019). The resulting contigs were then polished using raw reads and Arrow from v.GCpp 1.0.0-cd36561 to improve base accuracy (https://github.com/PacificBiosciences/gcpp) resulting in a consensus quality value of 39.7, corresponding to 99.99% base accuracy. Scaffolding was performed using SSPACE-longreads v.1.0 (Boetzer and Pirovano 2014). To assess the assembly completeness, we performed Benchmarking Universal Single-Copy Orthologs (BUSCO v5.4.2; Manni et al. 2021) analysis with the fungi_odb10 lineage dataset. Illumina sequencing reads from TN2 and LB22.1 were quality-filtered and adapter clipped using Trimmomatic v.0.36 (Bolger et al. 2014), with the following settings: LEADING:7, TRAILING:7, SLIDINGWINDOW:10:20, and MINLEN:140. SPAdes v.3.13.0 (Bankevich et al. 2012) was used to assemble the quality-filtered reads with the careful option and automatic read coverage cutoff after optimizing the multiple Kmer combination. To assess the assembly completeness of the genomes, we performed Benchmarking Universal Single-Copy Orthologs (BUSCO v.5.4.2; Manni et al. 2021) analysis with the fungi_odb10 lineage dataset. Additionally, the package tidk v.0.2.63 (Brown et al. 2025) was used with the search mode to identify the telomeric repeat "CCCTAA" in 1 kb windows. The genomes were screened for contamination using FCS-GX (Galaxy Version 0.5.5 + galaxy1), and no significant contamination was detected above the default thresholds. Most contigs were confidently assigned to *P. ampelicida* or to fungi and contigs with low coverage or ambiguous matches with no-fungal taxa were regarded as repetitive or low complex rather than contamination. Commands for all steps in the bioinformatic pipeline are presented in Supplementary File 1.

Variant analysis

Quality-filtered reads from the isolates TN2 and LB22.1 were mapped in a paired-end mode to the genome of the isolate GW18.1 using default parameters in BWA v.0.7.17 (Li and Durbin 2009). PCR and optical duplicates were removed with Picard tools v.2.0.1 (http://broadinstitute.github.io/picard/). HaplotypeCaller (GATK v.4.0.12.0; McKenna et al. 2010) was used to call sequence variants between the isolates using the parameters --ploidy 1 --min_base_quality_score 20. The variants were normalized using BCFtools norm v.1.9-94-g9589876 (Danecek et al. 2021) using the option -m-any. The SNP and small INDEL variants up to 50 bp were extracted using BCFtools view. The functional impact of SNPs and small INDELS was predicted with SnpEff v.5.1 (Cingolani et al. 2012) using default parameters.

RNA-seq analysis

Total RNA extraction from *P. ampelicida* GW18.1 in vitro culture, along with inoculated and mock-inoculated leaves (Bettinelli et al. 2023a) of *V. vinifera* cultivar "Pinot noir," was performed according to the CTAB protocol of Amrine et al. (2015). Stranded mRNA sequencing libraries (KAPA Stranded mRNA-Seq Kit. Roche, Switzerland), quality control, and quantification were performed at the Sequencing and Genotyping Platform of FEM (San Michele all'Adige, Italy). The sequencing was carried out on an Illumina Novaseq 6000 platform (Illumina, CA-USA) with paired-end runs of 2×150 bps at CIBIO Sequencing platform (Trento, Italy). RNA-seq reads were quality-filtered and adapter-clipped using Trimmomatic v.0.36 (Bolger et al. 2014), with the following settings: LEADING:7. TRAILING:7. SLIDINGWINDOW: 10:20. and MINLEN:36. Quality-trimmed reads from the pure fungi were then mapped to the *P. ampelicida* genome assembly. For the grapevine inoculated and mock-inoculated samples, reads were mapped to a combined reference of the *V. vinifera* (VITVvi_vPinNoir123_v1.0) and *P. ampelicida* genomes using HISAT2 v2.1.0 (Kim et al. 2019) with the very-sensitive option.

Functional annotation and trophic lifestyle inference

Repeat model libraries were predicted for *P. ampelicida* using RepeatModeler v.open-1.0.11 (Smit et al. 2015b) with default parameters. To mask the identified repeats RepeatMasker v.open-4.0.6. (Smit et al. 2015a) was employed along with the known fungal model libraries in the RepBase (v.20160829). For gene model prediction BRAKER1 was used with the option –fungus (Hoff et al. 2016). The Augustus v.3.2.1 (Stanke et al. 2006) version was used to train the models based on the alignment of RNAseq data on the assembled genome. The HISAT2 v2.1.0 (Kim et al. 2019) tool with the very-sensitive option was employed to align RNA-seq data on the assembled genome. The alignment was converted to bam, sorted by genomic coordinates, and indexed and for BRAKER1 using samtools-1.3.1 (Li et al. 2009). The predicted proteins were annotated based on the similarity to conserved domains in the Pfam database (Finn et al. 2016). For functional annotation, various databases and parameters (Supplementary Table 1) were used. CAZymes were annotated using dbCAN3 (Zheng et al. 2023), keeping only genes annotated with at least 2 of the 3 algorithms. Signal peptides were identified using SignalP 5.0 (Almagro Armenteros et al. 2019), and proteins with annotation in both SignalP5 and dbCAN3 databases were annotated as secreted CAZymes. Secondary metabolite clusters were annotated using antiSMASH 6.0 (Blin et al. 2021), while peroxidases were annotated using a specialized database for fungi, fPoxDB (Choi et al. 2014). Cytochrome P450 proteins were annotated using CYPED 6.0 (Sirim et al. 2009). Next, proteins involved in transportation functions were annotated using TCDB (Saier et al. 2006, 2016). Finally, proteins with signal peptides were analyzed for transmembrane (TM) domains with TMHMM 2.0 (Krogh et al. 2001).

Proteins with no predicted TM domain in the first 60 amino acids or no more than 2 TMs in total were used as input for effectorP3 (Han et al. 2022). These were used to annotate effector proteins as apoplastic, cytoplasmic, or with dual localization based on the probability values obtained with the software. If the difference between the probabilities was lower than 0.1, the effector protein was annotated as dual localization. The trophic lifestyle prediction of the organisms in this analysis was performed using CATASThrophy (Hane et al. 2020) with default parameters using the predicted protein of the species.

Comparative genomics

Genomes and gene annotations from the 4 *P. ampelicida* isolates (GW18.1, TN2, LB22.1, PA1) were compared to those of ascomycete species listed in Supplementary Table 2. Several *Phyllosticta* species with different levels of pathogenicity were included in the analysis. Additionally, 11 other species responsible for different plant diseases were used for functional comparison. Finally, the basidiomycetes *Fomitiporia mediterranea* and *Stereum hirsutum* along with the nonpathogenic species *Saccharomyces cerevisiae* were used as outgroups. The predicted proteins of all the genomes were used as input for OrthoFinder v.2.5.4 using default parameters. A total of 1,098 Single Copy Orthologs obtained were aligned using MUSCLE v.5.1 (Edgar 2004) with the option "-maxiters 16." The concatenated alignments were cleaned with Gblocks v.0.91b (Castresana 2000) to keep informative regions of the alignments using the default parameters. The cleaned alignments were used to optimize the evolutionary model using ModelTest-NG v.0.1.7 (Darriba et al. 2020). The maximum likelihood tree of the species was created with RAxML-NG v.0.9.0 (Kozlov et al. 2019), using the parsed alignment, and the optimized evolutionary model "LG + I + G4 + F" with the options "--tree pars{10} --bs-trees 100." The clock-calibrated tree was constructed using BEAST v.2.7.6 (Bouckaert et al. 2019). The parsed alignment was prepared with BEAUti v2.7.6 (Bouckaert et al. 2019). Calibration points were set for the ascomycetes crown to 588 million years ago (Mya) (Beimforde et al. 2014) with a normal distribution, and the dothideomycetes group set to 350 Mya (Beimforde et al. 2014) with a normal distribution. Six independent Markov chain Monte Carlo runs of 10,000,000 generations were used after confirming convergence (ESS > 200) using LogAnalyser v2.7.6. The LG substitution model with 4 gamma categories, and the Birth-Death model was used. Tree sampling was done every 1,000 generations. LogCombiner v.2.7.6 (Bouckaert et al. 2019) was used to combine the resulting log and tree files. TreeAnnotator v2.7.6 (Bouckaert et al. 2019) was used to generate the maximum clade credibility tree using a burn-in of 10% of generations. Figtree (Rambaut 2018) was used to plot and annotate the phylogenetic trees.

Gene family expansion and contraction analysis

The predicted proteins in all the genomes were clustered following the methods described in Garcia et al. (2024a). The resulting file was prepared for CAFE using the script cafetutorial_mcl2rawcafe.py at https://github.com/hahnlab/cafe_tutorial/tree/main/python_scripts. The resulting file was used to run CAFE with the option "-P 0.0100," an estimated lambda value of 0.00063887950005574, and the clock-calibrated tree. Families with significant rates of gain or loss of genes (P-value < 0.01) were extracted. CafePlotter (https://github.com/moshi4/CafePlotter) was used to annotate the clock-calibrated tree with the number of families expanding and contracting. A Fisher's exact test was used to obtain the functions that were significantly enriched in the expanded and contracted families of the species of interest.

Results and discussion

A highly contiguous *P. ampelicida* genome assembly

PacBio CLR sequences of *P. ampelicida* GW18.1 were de novo assembled into 22 scaffolds with an N50 of 1.9 Mb, 99.99% of consensus accuracy. These metrics indicate a high-quality assembly, with room for improvement through the use of more accurate or complementary sequencing technologies (Chin et al. 2016; Rhie et al. 2021). In the addition to the previous statistics, the obtained BUSCO completeness score of 99.3% confirms the completeness of the assembly. Four of the scaffolds were complete chromosomes and 12 were chromosome arms based on the presence of telomeric repeats (Supplementary Table 3). The genome spans a total of 35.6 Mb (Table 1) that is about 16.7% larger than the draft genome reported by Eichmeier et al. (30.5 Mb, Eichmeier et al. 2022) and the largest *Phyllosticta* genome sequenced to date (Guarnaccia et al. 2019; Rodrigues et al. 2019; van Ingen-Buijs et al. 2024). The increase in size is likely due to the use of long-read sequencing, which improves contiguity and captures repetitive regions more effectively than short-read approaches (Chin et al. 2016). Supporting this, repetitive sequences accounted for 23% of the genome (Supplementary Table 4), much higher than in other grapevine pathogens (e.g. 5% for *Neofusicoccum parvum*; Garcia et al. 2024b). Of the 8 Mb of repeats, 92% were interspersed, with 87% unclassified and 13% identified as transposable elements, dominated by long terminal repeats (74%). Short tandem repeats comprised the remaining 8%. Gene prediction identified 10,289 coding DNA sequences, closely matching the 10,691 previously reported for this species (Eichmeier et al. 2022). Of these, nearly 80% (8,115) matched annotated genes, with 75% (7,704) carrying complete Pfam domains (Table 2). Additionally, signal peptide predictions indicate that about 7% of the proteins may be secreted.

Sequence and structural variation across *P. ampelicida* genomes

To begin exploring intraspecific genetic diversity, we sequenced 2 Italian *P. ampelicida* isolates using short-read technology and analyzed them alongside the available genome of the Spanish PA1 strain (Eichmeier et al. 2022). Despite higher fragmentation, the de novo Illumina assemblies of TN2 and LB22.1 showed high completeness (~99.3% BUSCO), comparable to the PacBio-assembled genome of GW18.1 (Table 1). Sequence variants smaller than 50 bp were identified by mapping Illumina reads onto the assembly of GW18.1.

TN2 and LB22.1 contained 88,862 and 89,134 variants relative to GW18.1, respectively (Supplementary Table 5a). The majority (91.2 ± 0.0001%) were 1 bp variants, of which 95.5% were SNPs and the remaining 4.5% were 1 bp indels. Variants between 2 to 10 bp and 11 to 50 bp accounted for 6.3 ± 0.002% and 2.5 ± 0.01%, respectively (Figure 2a, Supplementary Table 5a). The cumulative variant length averaged 150.4 ± 0.09 kbp per isolate. Single nucleotide variants (including SNPs and 1 bp indels) contributed 54.0 ± 0.1% of the total (Fig. 2b, Supplementary Table 5b).

The high genetic similarity between the 2 Italian strains, whose geographical sampling sites are about 150 km apart, likely reflects clonal expansion from a recent common ancestor. Warmer winter temperatures may further suppress sexual reproduction, as observed in *Plasmopara viticola* (Santos et al. 2020), limiting opportunities for genetic recombination. This low diversity could reduce

Table 1. Summary of genome sequencing statistics of *P. ampelicida* isolates.

Sequencing technology	GW18.1 PacBio CLR	LB22.1 Illumina NovaSeq	TN2 Illumina NovaSeq	PA1[a] Illumina MiniSeq
Genome size (Mb)	35.6	33.1	33.1	30.55
Scaffolds	22	11,063	10,944	6,675
N50 length	1.9 Mbp	90.2 kbp	85.3 kbp	20.6 kbp
N90 Index (or L90)	15	549	580	1.768
BUSCO completeness[b]	99.3%	99.2%	99.3%	98.8%
Repeat content (Mbp)	8.0 (22.6%)	5.4 (16.4%)	5.4 (16.4%)	3.1 (10.2%)
N. CDSs	10,289	8,804	8,802	7,983[c]
Mean protein size (AA)	543	505	505	509[c]
Sequencing depth	653×	90×	85×	60×
Genome coverage	100	99.07%	99.07%	NA

[a] Published in Eichmeier et al. (2022).
[b] Percentage of complete BUSCO peptides found in the assembled genomes.
[c] Numbers calculated based on a new gene annotation made in this work for the previously published genome.

Table 2. Summary of predicted protein-coding genes in *P. ampelicida* GW18.1, categorized by annotated functions and total number of genes affected by high-impact variants.

	Total		Affected by high impact variants	
Category	Count	%	Count	%
Total genes	10,289		354	3.40%
Genes without functional annotation	2,196	21.34	125	35.31%
Genes with functional annotation	8,093	78.66	229	64.69%
PFAM	7,704	74.88	212	2.80%
Transporters	2,190	21.28	25	1.10%
Cytochrome P450 proteins	54	0.52	2	3.70%
Signal peptides	718	6.98	18	2.50%
CAZymes	314	3.05	5	1.60%
Secreted CAZymes	169	1.64	2	1.20%
Secondary metabolites involved genes	277	2.69	7	2.50%
Peroxidases	35	0.34	1	2.90%

the pathogen's evolutionary potential, increasing its susceptibility to control measures such as fungicides or host resistance. However, these genomes were assembled using short-read sequencing, which may limit the detection of longer variants.

Variant density in repeat and gene space did not show substantial differences between the Italian strains (Fig. 2c). As expected, variants were more frequent in repeat regions than in gene space in both isolates (2.7 ± 0.01 vs 1.5 ± 0.003 variants/kbp) (Supplementary Table 5c). Assuming a uniform distribution of the total variants across the chromosome windows, the average number of variants was significantly lower than expected at chromosome ends (Supplementary Fig. 1; Chi-squared *P*-value < 1.03e−3), corresponding to telomeric regions (Supplementary Table 3), though other genomic windows emerged as potential evolutionary hot spots (Supplementary Fig. 1). The lower-than-expected number of variants toward the telomeres could be associated with low mapping quality or reads mapping to multiple regions due to the repetitive nature of telomeric and subtelomeric regions (Treangen and Salzberg 2012). SNPs were more frequent than indels, with marked positional differences. In repeat regions, SNPs were 3 times more abundant than indels, while in gene space, they were 18 times more frequent (Fig. 2c). Given that indels are more likely to disrupt gene function, their lower density in gene space than SPNs likely reflects stronger selective constraints on coding regions. This pattern aligns with trends observed in other fungal pathogens, where coding regions are overall conserved, while repeat-rich regions serve as reservoirs for structural variation and adaptive evolution.

Variants were classified based on their predicted impact on coding sequences: low (mostly synonymous mutations), moderate (multiple of 3 insertions or deletions that would change a full codon), or high (e.g. premature stop codons or frameshift mutations; Supplementary Table 6). Most affected genes carried low-impact ($58.6 \pm 0.05\%$) or moderate-impact ($46.8 \pm 0.05\%$) variants, while only $3.4 \pm 0.05\%$ were affected by high-impact mutations, with some of them affecting only one of the isolates (Supplementary Tables 5d, 6, 7). Low-impact and moderate-impact variants were 285 and 12 times more common in SNPs than in indels, respectively. In contrast, high-impact variants were twice as likely to be caused by indels (4.0 ± 0.03 vs 2.0 ± 0.02 variants per 100 genes) (Fig. 2d, Supplementary Table 5e).

Comparative analysis of putative pathogenicity and virulence factor genes

Comparative analysis of family sizes of putative virulence factors was performed between *Phyllosticta* species and plant-pathogenic ascomycetes, focusing on genes potentially associated with pathogenicity and virulence, such as those encoding CAZymes, cytochrome P450s, biosynthetic gene clusters (BGCs), peroxidases, and cellular transporters. The comparisons included Phyllosticta species with diverse lifestyles: *P. citricarpa*, a major citrus pathogen (Timmer et al. 2000); *P. capitalensis*, a widespread citrus endophyte and a weak pathogen in other hosts (Silva et al. 2008; Wikee et al. 2013; Cheng et al. 2019); *P. citrichinaensis*, a minor citrus pathogen in China which exhibits genomic features of both endophytes and pathogens (Buijs et al. 2021); and the closely related *P. citribraziliensis*, an endophyte found in asymptomatic citrus leaves in Brazil (Glienke et al. 2011). We also included a nonpathogenic ascomycete (*S. cerevisiae*) and 2 wood-rotting basidiomycetes associated with esca (*F. mediterranea* and *S. hirsutum*), another important grapevine disease.

Overall, the abundance of virulence factor genes confirmed that the Italian strains LB22.1 and TN2 are highly similar to each other and more closely related to the Spanish *P. ampelicida* PA1 strain than to the German strain GW18.1. At the interspecific level, *P. ampelicida* appears more similar to *P. capitalensis* than to *P. citrichinaensis*, *P. citribraziliensis*, or *P. citricarpa* (Sui et al. 2023). Additionally, certain putative virulence factors, such as GH16, AA1, and some secreted CAZymes, were slightly more abundant

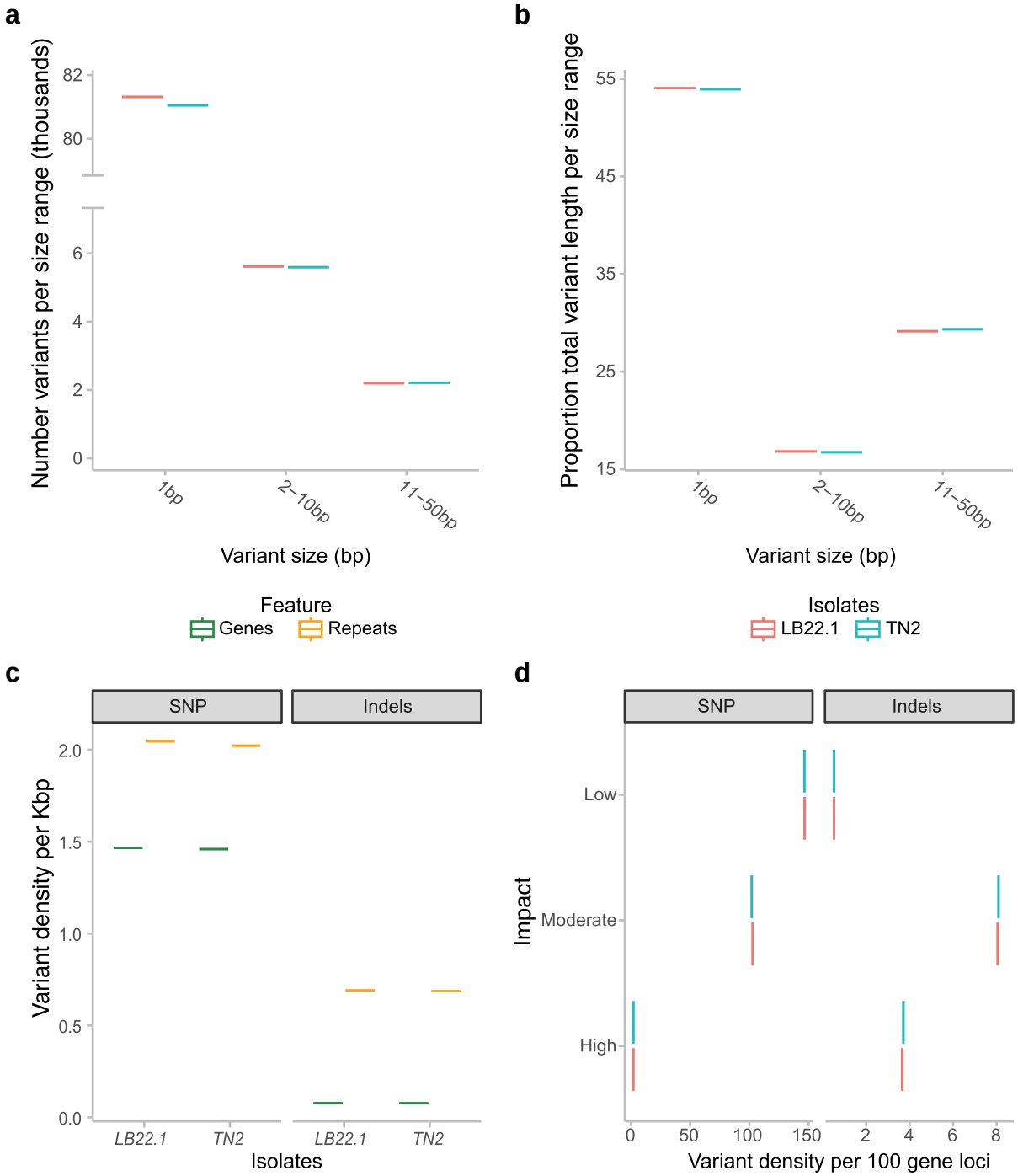

Fig. 2. Variant analysis of *P. ampelicida* isolates. a) Count of variants per size range. b) Proportion of total variant length per size range. c) Variant density in gene space compared to repeat space. d) Number of variants per 100 gene loci and their effect level based on the SNPeff prediction.

in *P. ampelicida* genomes compared to other Phyllosticta species. However, most other virulence factors analyzed showed similar or lower abundance in *P. ampelicida* relative to the rest (Fig. 3).

Repertoire of CAZymes

Plant cell wall polysaccharides play a dual role in plant–pathogen interactions, serving as both barriers and nutrient sources (Cantu et al. 2008). CAZymes that target the plant cell walls facilitate these interactions by degrading cellulose, hemicellulose, pectin, and other components, enabling host invasion and nutrient acquisition (Bruno et al. 2006; Ospina-Giraldo et al. 2010; Kubicek et al. 2014; Barrett et al. 2020). A dbCAN3 analysis identified 314 putative CAZyme genes in *P. ampelicida*, ~3% of the total number of genes in the genome (Table 2). This is consistent with other *Phyllosticta* species and dothideomycetes, which typically encode 300 to 400 CAZyme genes (Saier et al. 2006; Ohm et al. 2012; Haridas et al. 2020; Buijs et al. 2021). The largest CAZyme families include glycoside hydrolases (GH, 161 genes), glycosyltransferases (GTs, 71 genes), and auxiliary activities (AAs, 59 genes). Smaller families include carbohydrate-binding modules (CBMs, 16 genes), carbohydrate esterases (CE, 16 genes), and polysaccharide lyases (PL, 7 genes) (Supplementary Fig. 2).

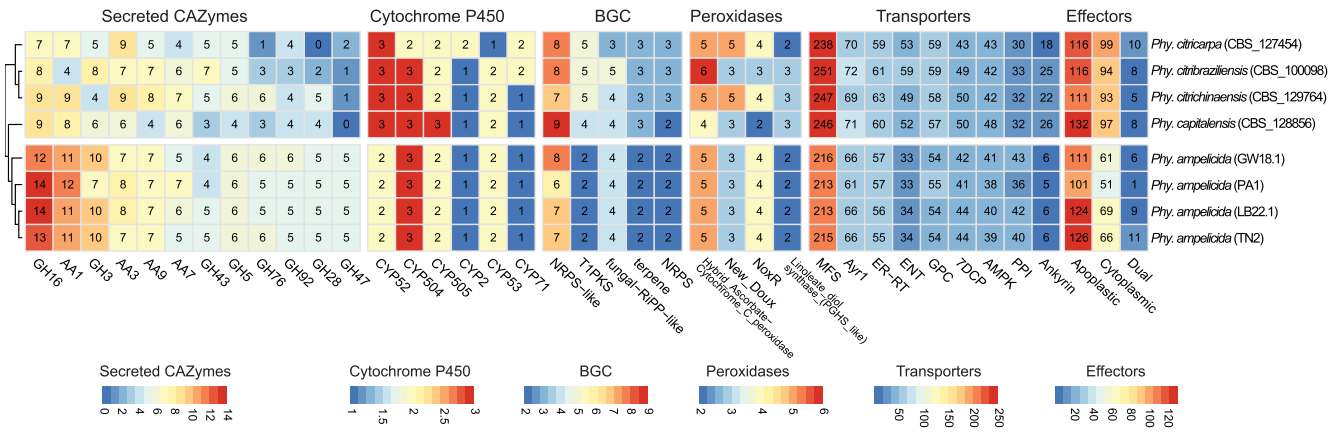

Fig. 3. Number of protein-coding genes annotated as secreted CAZymes, P450s, secondary metabolism, peroxidases, transporters, and effectorP prediction. The heatmap includes only the annotations with the highest number of genes across Phyllosticta genomes. Overrepresented and underrepresented domains are depicted as Z-scores for each family.

Table 3. Putative secreted CAZymes in *P. ampelicida* classified by family.

CAZymes	Total	Secreted	%
AA	59	39	66.10
CBM	16	8	50.00
CE	16	11	68.75
GH	161	106	65.84
GT	71	7	9.86
PL	7	6	85.71

Among *Phyllosticta* species, *P. ampelicida* possesses the smallest set of genes encoding CAZymes, particularly the CBMs, with only 16 genes compared to 34 in *P. citribraziliensis* and 45 in *P. capitalensis*. CBMs facilitate carbohydrate recognition and enhance enzymatic activity (Gilbert et al. 2013; Várnai et al. 2014). Similarly, *P. ampelicida* has fewer GHs (161 vs ~177 in other *Phyllosticta* species) and GTs (71 vs ~81). Despite these differences, the CAZymes repertoire remains similar across *Phyllosticta* species regardless of their lifestyle (Wang et al. 2020; Buijs et al. 2021). Genome-based prediction of the *P. ampelicida* CAZyme secretome, an additional indicator of cell wall-degrading enzyme activity with potential implications during pathogen-plant host interactions, suggests that 50 to 85% of CAZyme proteins are secreted, except for GTs (Table 3; Fig. 3, Supplementary Table 8). The most abundant secreted families target hemicellulose (GH16), cellulose (GH3), and lignin (AA1 laccases). Other major families include AA3 (supporting lignocellulose degradation) and copper-dependent AA9 proteins (Van Den Brink and De Vries 2011; Moses et al. 2016; Sützl et al. 2018; Drula et al. 2022).

Interestingly, *P. ampelicida* has the highest number of predicted secreted CAZymes (~180) among *Phyllosticta* species, surpassing *P. citricarpa* (109) and *P. citrichinaensis* (158) (Fig. 3). For instance, it possesses 14 secreted GH16 proteins—twice as many as *P. citricarpa*. Despite this, intra-species variation is minimal, with >90% of secreted CAZyme families showing no differences across isolates. However, the Spanish PA1 isolate exhibits notable reductions in GH3 genes (7 vs 10 in other isolates) and AA11 lytic polysaccharide monooxygenases (2 vs 4).

Beyond *Phyllosticta*, pathogenic ascomycetes exhibit a larger CAZyme repertoire, with 114 CAZyme families in *Phaeoacremonium minimum* and 89 in *Elsinoe ampelina*, compared to 56 to 69 in *Phyllosticta*. These species are enriched in AA7, AA9, and AA3 auxiliary enzymes and GH families targeting pectin (GH43, GH28), hemicellulose (GH16), cellulose (GH3), and chitin (GH18) (Chen et al. 2020; Fig. 4). The largest families include CBM1 (cellulose-binding) and CE5 (cutinases targeting the plant cuticle). In contrast, *S. cerevisiae* has few CAZymes, while wood-decaying basidiomycetes (*F. mediterranea*, *S. hirsutum*) have CAZymes numbers comparable to pathogenic ascomycetes.

Inference of trophic lifestyle based on CAZyme repertoire

CATAstrophy (Hane et al. 2020) categorizes species based on their predicted ecological roles through comparative genomic studies of CAZymes, providing a detailed understanding of their trophic strategies. This classification identifies 5 ecological groups: monomertrophs, which metabolize simple sugars and include biotrophs and symbionts (both haustorial and nonhaustorial species); polymertrophs, which metabolize complex sugars and encompass necrotrophs, further divided into narrow and broad host-range categories, with the latter requiring a richer CAZyme repertoire for adaptation to multiple hosts; mesotrophs, corresponding to hemibiotrophs, which are further distinguished as intracellular or extracellular based on their adaptation to host invasion, linked to their ability to feed through appressoria-like structures; and vasculartrophs, which are wilt-like pathogens lacking a specific trophic lifestyle but possessing a CAZyme repertoire more similar to broad host-range polymertrophs.

Species within Phyllostictaceae span multiple trophic classifications, with *P. ampelicida* showing an intermediate profile between monomertrophy (1.0), extracellular-mesotrophy (0.89), and saprotrophy (0.81), suggesting a mixed trophic strategy (Supplementary Table 9). The number of predicted secreted effectors is consistent with an extracellular-mesotrophic lifestyle, as also supported by its CAZyme profile. The number of predicted secreted effectors is consistent with an extracellular mesotrophic lifestyle, as further supported by the CAZyme profile. *P. ampelicida* has been described to grow subcuticularly, surrounding epidermal cells during the hemibiotrophic phase of host tissue invasion (Ullrich et al. 2009). However, the boundary between mesotrophs (typically hemibiotrophs) and monomertrophs (biotrophs) remains unclear (De Silva et al. 2016; Précigout et al. 2020). *P. ampelicida* has been traditionally classified as a hemibiotroph, exhibiting biotrophic-like features such as a prolonged latent phase exceeding 21 d, followed by a necrotrophic phase

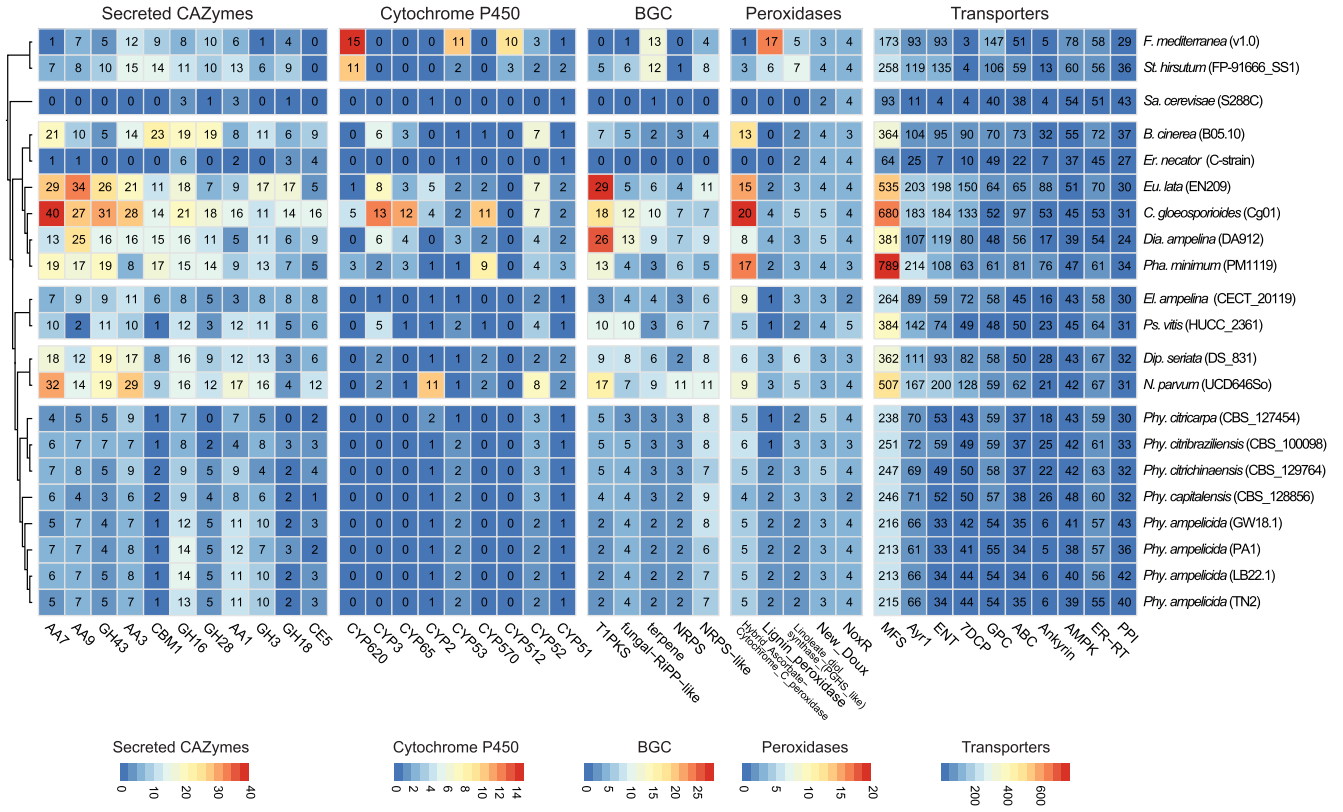

Fig. 4. Number of protein-coding genes annotated as secreted CAZymes, P450s, secondary metabolism, peroxidases and transporters. The heatmap includes only the annotations with the highest number of genes across all genomes. Overrepresented and underrepresented domains are depicted as Z-scores for each family.

characterized by tissue damage and symptom development (Bettinelli et al. 2023a).

Cytochrome P450 monooxygenases

Cytochrome P450 monooxygenases (CYPs) are a diverse superfamily of heme-containing enzymes involved in the metabolism of endogenous and xenobiotic compounds. In fungi, they play a crucial role in adaptation to ecological niches by contributing to secondary metabolite biosynthesis, nutrient utilization, pathogenesis, resistance to drug and oxidative stress and plant immune responses inhibition (Črešnar and Petrič 2011; Chen et al. 2014a; Durairaj et al. 2016; Fu et al. 2025). In *P. ampelicida*, the CYP repertoire is conserved across isolates, with all sharing an identical repertoire of 17 genes across 12 families. Similarly, *Phyllosticta* species exhibit minimal variation, with CYP gene counts ranging from 17 in *P. ampelicida* to 19 in *P. capitalensis*, *P. citribraziliensis*, and *P. citrichinaensis*. All species share the same 12 families, except *P. citrichinaensis*, which has an additional CYP83 family (Supplementary Table 8).

The largest CYP families in *Phyllosticta* include CYP504, an enzyme involved in phenylacetate catabolism (Mingot et al. 1999); CYP52, which aids in alkane and fatty acid assimilation (Ortiz-Álvarez et al. 2020); CYP505, responsible for fatty acid oxidation (Nakayama et al. 1996); and CYP53, which plays a role in detoxification (Moktali et al. 2012; Akapo et al. 2019). Each family contains 1 to 3 genes, with little variation among species. However, *P. citricarpa*, the most phylogenetically distant species, exhibits distinct differences, possessing an additional CYP2 gene while lacking one gene each in CYP53 and CYP504. Additionally, *P. citricarpa* and *P. citribraziliensis* share an extra CYP71 gene.

Phyllosticta species, along with *E. ampelina*, have the smallest number of CYPs and the fewest identified families, in contrast, Colletotrichum *gloeosporioides* has the largest number of CYPs, with 121 genes spanning 35 families (Fig. 4). Other pathogenic species exhibit an intermediate number of CYPs, ranging from 31 genes in *Diplodia seriata* and *Pseudocercospora vitis* to 58 genes in *Eutypa lata*. Many CYP families in *Phyllosticta*, such as CYP51 and CYP61, are essential for ergosterol biosynthesis and cell wall integrity (Črešnar and Petrič 2011; Chen et al. 2014b).

Peroxidases

Peroxidases, a group of oxidoreductases including NAD(P)H oxidase, catalase, and lignin peroxidase, play key roles in lignin degradation, detoxification, and ROS regulation. These enzymes contribute to carbon recycling and fungal pathogenicity (Choi et al. 2014; Mir et al. 2015; Jia et al. 2023). *P. ampelicida* possesses 35 peroxidase genes (34 in strain PA1), distributed across 16 families, each containing 1 to 5 genes. Intraspecies variation is minimal, occurring only in the Spanish PA1 strain, which differs from other *P. ampelicida* strains and *Phyllosticta* species by a reduced set of atypical 2-cysteine peroxiredoxins. PA1 has only one type II and type V gene instead of 2, and it lacks the single type Q and BCP genes typically present in the genus. However, it uniquely possesses the respiratory burst oxidase homolog-type NADPH oxidase gene, which is found in all *Phyllosticta* species but absent in other *P. ampelicida* strains.

Among *Phyllosticta* species, the number of peroxidase genes ranges from 33 in *P. capitalensis* to 38 in *P. citrichinaensis*, with 16 families identified in each species. The largest is the hybrid ascorbate-cytochrome C peroxidase family, averaging 5 ± 0.3

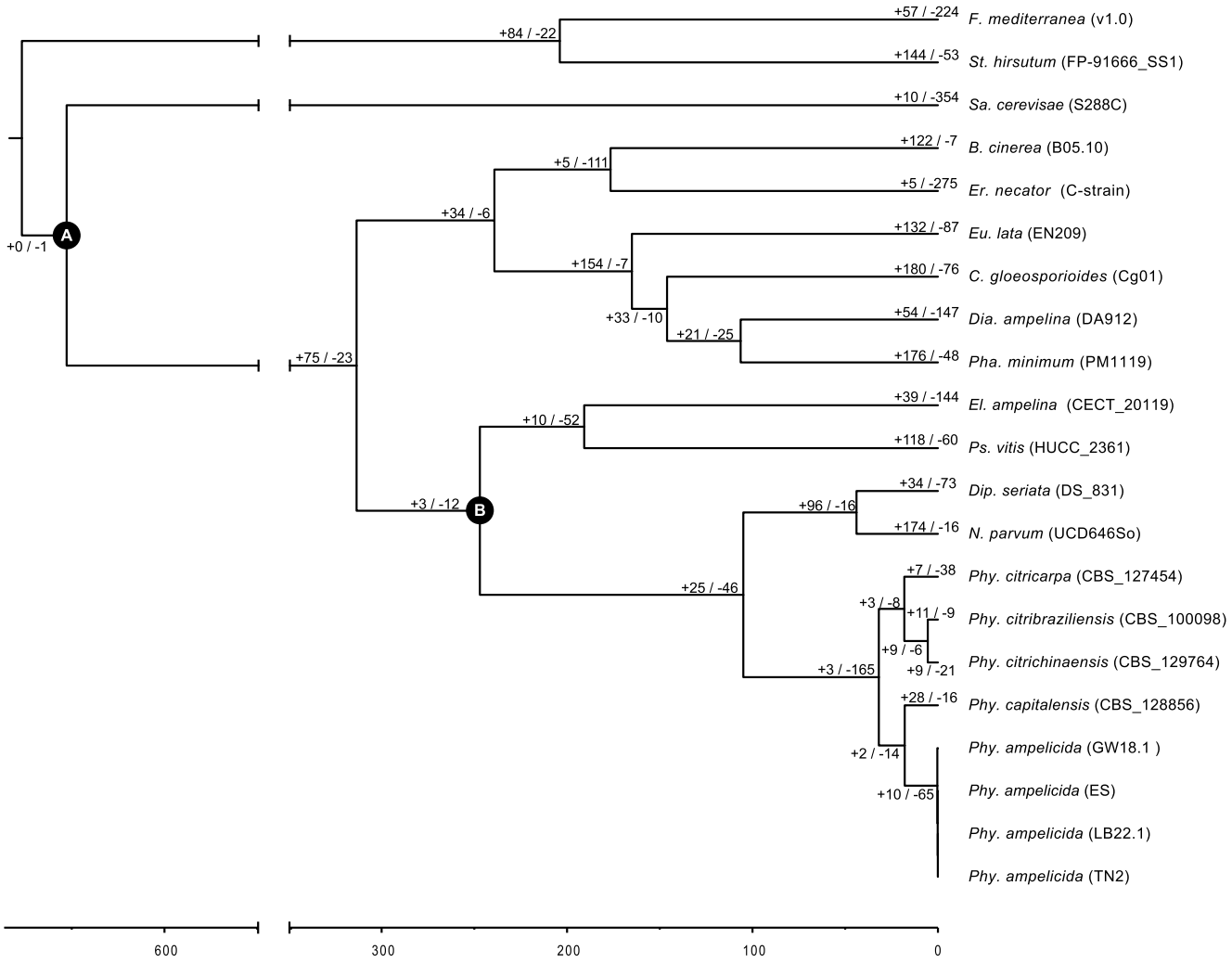

Fig. 5. Clock-calibrated phylogenetic tree with estimated times of divergence in Mya and numbers of expanded and contracted gene families. Clock-calibrated phylogenetic tree with analysis of gene family expansion and contraction. The length of the branches represents divergence times in million years. Calibration point a) at ascomycete crown. Calibration point b) at the dothideomycetes divergence. Positive and negative numbers represent families under expansion and contraction, respectively, as determined by gene family evolution analysis CAFE.

genes per species. The most notable differences are found in the NADPH oxidase (Nox) enzyme family, which synthesizes ROS for cell defense and signaling (O'Brien et al. 2012). While NoxA and NoxB are conserved across the genus, *P. ampelicida* is the only species to possess a NoxC gene, a rare subfamily with an unclear biological function (Takemoto and Scott 2023). Additionally, the 2 endophytic species, *P. citribraziliensis* and *P. capitalensis*, have a reduced set of NoxR regulatory genes.

Compared to other grapevine pathogens, *Phyllosticta* species have the fewest peroxidase genes, except for *Erysiphe necator* (22 genes). Other pathogens possess larger repertoires, ranging from 47 in *E. ampelina* to 58 in *N. parvum*, with *C. gloeosporioides* having the most (71 genes; Fig. 4). Across these species, heme peroxidases are the predominant type, with the hybrid ascorbate-cytochrome C peroxidase family being particularly abundant. These enzyme families are quite large in pathogens such as *C. gloeosporioides*, *P. minimum*, *E. lata*, and *Botrytis cinerea*, where their numbers range from 13 to 20 genes.

BGCs and secondary metabolism potential

Fungal secondary metabolites are essential for growth, development, pathogenesis, nutrient acquisition, and ecological interactions (Keller 2019; Yang et al. 2024). In fungal genomes, genes encoding enzymes involved in biosynthesis, modification, and transport of secondary metabolites are organized into BGCs, which typically include core biosynthetic genes, tailoring enzymes, regulatory transcription factors, and transporters (Brakhage 2013; Keller 2019). *P. ampelicida* strains share a small core set of BGCs. Italian strains TN2 and LB22.1 have 20 BGCs each, while the Spanish strain PA1, which lacks the isocyanide cluster and has only 6 NRPS-like clusters, has the fewest (18). The GW18.1 strain, with 8 NRPS-like clusters, has the highest number (21) (Supplementary Table 8). Within *Phyllosticta*, *P. ampelicida* has the fewest BGCs, whereas *P. citrichinaensis* and *P. citribraziliensis* contain 25 and 28 clusters, respectively. *P. ampelicida* lacks the NRP-metallophore BGC and has the smallest type I polyketide synthase (T1PKS) cluster, with an overall moderate reduction in BGCs. Despite this, a minimal core set of BGCs is shared within the genus.

Secondary metabolite diversity varies widely among grapevine pathogens (Supplementary Table 8). *Diaporthe ampelina* has the highest number of BGCs (81), followed by *E. lata* (69) and *N. parvum* (67). In contrast, *Phyllosticta*, *E. ampelina* (23), and *B. cinerea* (25) have fewer. Half of the BGCs are species-specific, while others, such as fungal-RiPP clusters, are found in only 2 species. Common grapevine pathogen BGCs (T3PKS, indole,

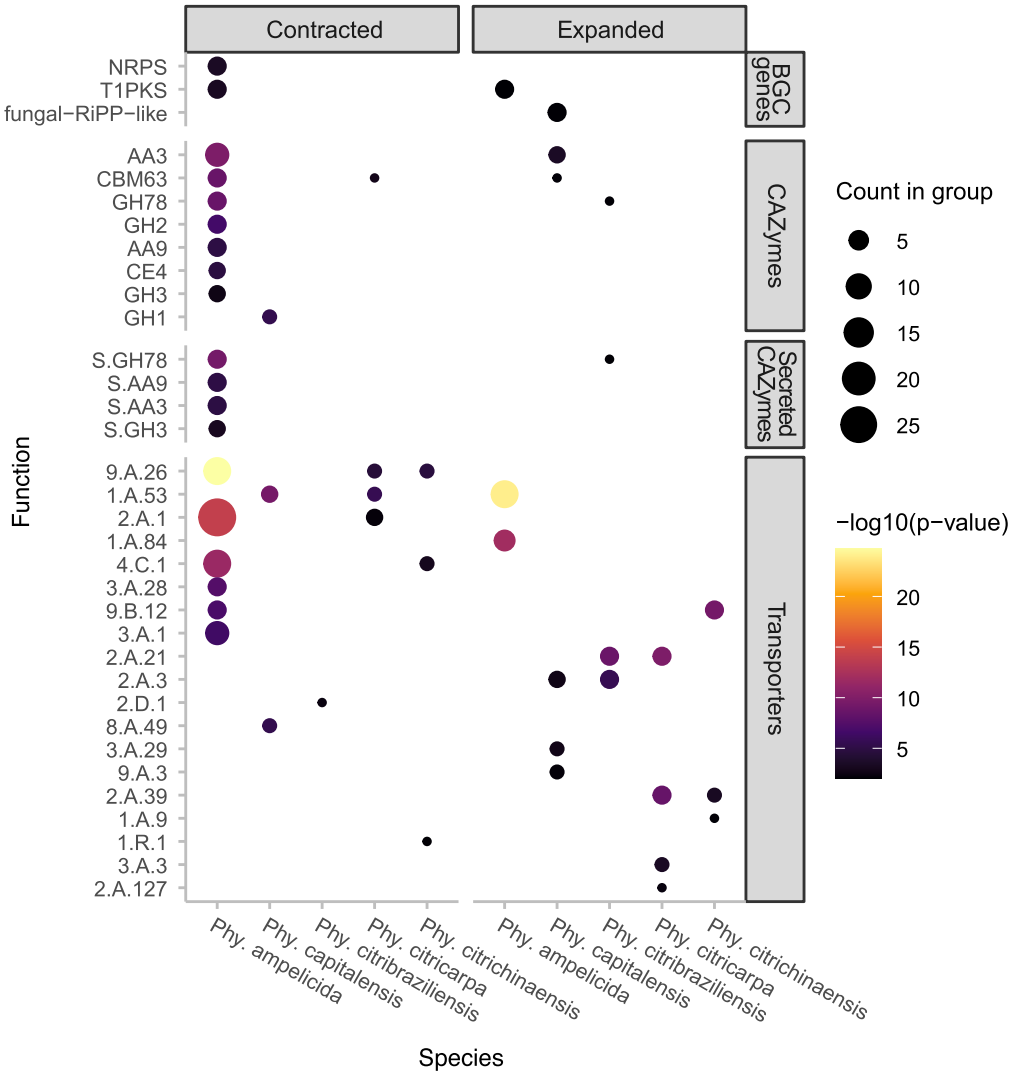

Fig. 6. Dotplot representing the genes enriched in the rapidly evolving families of the Phyllosticta species presented in this work. The dot size represents the number of genes in each category and the color scale the strength of the enrichment based on the *P*-value. The gene putative functions are displayed on the left axis and the functional categories on the right.

NRPS|T1PKS-like) are absent in *Phyllosticta*, while beta-lactone, isocyanide, and NRP-metallophore|NRPS clusters are common in *Phyllosticta* but rare in other pathogens.

Transporters

Membrane transporters contribute to virulence by secreting secondary metabolites and toxins while excluding host-derived antimicrobial compounds (Denny and VanEtten 1983; Denny et al. 1987). Among *P. ampelicida* isolates, transporter variation is minimal (Supplementary Table 8), with the major facilitator superfamily (MFS) being the largest. At the genus level, *P. ampelicida* has the fewest transporters, with the numbers of members being reduced across all major families. Compared to other grapevine pathogens, *Phyllosticta* species exhibit fewer transporters, particularly within the MFS family. Overall, the clade including *E. lata*, *C. gloeosporioides*, *D. ampelina*, and *P. minimum* has the highest number of identified virulence factors, while *Phyllosticta* possesses relatively few.

Putative fungicide targets

P. ampelicida exhibits insensitivity to Cidely, a fungicide targeting grapevine powdery mildew. Cidely combines Cyflufenamid (FRAC Code U6, unknown mode of action) and Difenoconazole (FRAC Group 3, demethylation inhibitor or sterol biosynthesis inhibitor), which disrupts ergosterol biosynthesis, essential for fungal cell membrane integrity. DMI resistance in fungi often stems from mutations in *CYP51*, encoding cytochrome P450 lanosterol C-14α demethylase. However, the gene Gb01.g2769 in the sequenced *P. ampelicida* GW18.1 lacks known fungicide resistance mutations, such as Y137F (Behr et al. 2012), F489L (Mair et al. 2020), M231T (Zhang et al. 2020), S509T (Arnold et al. 2024), Y144F/Y144H (Pereira et al. 2017), I387M (Muellender et al. 2021), and G207A (Wang et al. 2021). This suggests its insensitivity to Cidely may stem from alternative mechanisms, such as enhanced efflux pump activity or increased *CYP51* accumulation (Jones et al. 2014).

Gene family expansion and contraction

To assess whether differences in putative virulence factor counts among species groups result from accelerated gene family evolution, we conducted a CAFE analysis (Mendes et al. 2021). This approach calculates gene birth and death rates within families to identify lineages with significant changes in gene family size.

First, single-copy orthologs were identified in predicted proteins across all genomes and used to build a clock-calibrated tree (Fig. 5), calibrated with ascomycetes crown age (588 Mya) and dothideomycetes divergence (350 Mya). Second, all predicted proteins were clustered into families, and gene family sizes were calculated. Both datasets were used to run the CAFE pipeline. *Phyllosticta* species exhibit a low expansion/contraction ratio, with only 3 significantly expanded and 165 significantly contracted gene families (Fig. 5). Specifically, the *P. ampelicida* lineage shows an overall contraction, with 10 expanded and 65 contracted gene families. In contrast, highly pathogenic species like *E. lata*, *P. minimum*, and *N. parvum* show at least 50% more expanding than contracting gene families. This difference may relate to *P. ampelicida* extended latent period, resembling biotrophic organisms (Bettinelli et al. 2023a), while the necrotrophic *E. lata*, *P. minimum*, and *N. parvum* exhibits high virulence. Another factor could be *P. ampelicida* narrow host range, restricted to Vitaceae (Szabó et al. 2023), compared to the broad host range of *E. lata*, *P. minimum*, and *N. parvum* (Garcia et al. 2021).

Genes from significantly expanded or contracted families were analyzed for functional enrichment (Fig. 6, Supplementary Table 10). In *P. citricarpa* and *P. citribraziliensis*, expansion is enriched for APC (amino acid-polyamine-organocation) superfamily transporters (2.A.39, 2.A.21, 2.A.3), which facilitate ion co- and counter-transport with amino acids, likely contributing to nutrient acquisition and other cellular processes (Jack et al. 2000). The 9.B.12 transporter family, linked to salt tolerance, is enriched in *P. citrichinaensis* expanding families. In *S. cerevisiae*, deletion of genes in this family increases NaCl sensitivity (Navarre 2000). In *P. capitalensis*, α-Type channels (1.A) are enriched in contracted families, while in *P. ampelicida*, they are enriched in expanding families. These ubiquitous transporters facilitate passive solute movement (Saier 2000). This is consistent with the initial and elongated biotrophic phase of *P. ampelicida* in the development of black rot in grapevine, where the fungus limits its interaction with few superficial cells (Kuo and Hoch 1996a; Ullrich et al. 2009). Expanding this kind of transporters possibly helps the fungi with a slow but steady development without spending many resources in the transport of nutrients. Additionally, the contracted families of *P. ampelicida* shows an enrichment for CAZymes, including GHs (GH78, GH2), CBMs (CBM63), and AA enzymes (AA3, AA9). These genes function in rhamnosidase and galactosidase activity, lignocellulose binding and degradation, and lytic polysaccharide monooxygenase activity, all associated with fungal degradation of plant cell walls. The contraction of these functions in *P. ampelicida* suggests a reduced ability to degrade plant material, particularly mature tissues with thickened cuticles and cell walls (Kuo and Hoch 1996b), especially when compared with highly pathogenic species like *E. lata*, and *N. parvum* where these groups of functions are enriched in the families under expansion (Morales-Cruz et al. 2015; Garcia et al. 2021).

Data availability

The sequencing data and genome assemblies for this project are available at NCBI (https://www.ncbi.nlm.nih.gov/bioproject/PRJNA1231451). The genome assemblies and gene models produced in this study are publicly available at Zenodo (https://zenodo.org/records/15264932). Dedicated genome browsers and BLAST tools are available at https://www.grapegenomics.com. The Supplementary material is available at G3 online.

Acknowledgments

We thank Drs. Rosa Figueroa-Balderas, Andrea Minio, and Noé Cochetel for their technical support and the UC Davis DNA Technologies Core for sequencing assistance.

Funding

D.C. was partially supported by the Ray Rossi Endowment in Viticulture and Enology and by the California Department of Food and Agriculture, California Fruit Tree, Nut Tree, and Grapevine Improvement Advisory Board (Grant# 20-1062-000-SA; 21-0427-000-SA; 22-1588-000-SA; 23-0706-000-SA). M.C., S.L.T., G.M., and S.M. were supported by Regione Lombardia (project 33 New Defense Strategies Against Black Rot in Grapevines: A Threat to Lombard Viticulture CUPG44I20000890003). P.B. was supported by the Agritech National Research Center and received funding from the European Union Next-Generation EU (PIANO NAZIONALE DI RIPRESA E RESILIENZA (PNRR)—MISSIONE 4 COMPONENTE 2, INVESTIMENTO 1.4—D.D. 1032 17/06/2022, CN00000022).

Conflicts of interest

The authors declare no conflict of interest.

Author contributions

Conceptualization: M.C., P.B., J.G., S.V., S.M., D.C. Formal analysis: M.C., P.B., J.G. Investigation: M.C., P.B., J.G., G.M. Resources: M.C., P.B., J.G., G.M., S.T., L.H., S.V., S.M., D.C. Data curation: J.G. Writing—original draft preparation: M.C., J.G., P.B., D.C. Writing—review and editing: M.C., P.B., J.G., S.T., L.H., S.V., S.M., D.C. Visualization: M.C., P.B., J.G. Supervision: M.C., S.V., S.M., D.C. Project administration: M.C., S.V., S.M., D.C. Funding acquisition: S.M., D.C. All authors have read and agreed to the published version of the manuscript.

Literature cited

Akapo OO *et al.* 2019. Distribution and diversity of cytochrome P450 monooxygenases in the fungal class Tremellomycetes. Int J Mol Sci. 20:2889. https://doi.org/10.3390/ijms20122889.

Almagro Armenteros JJ *et al.* 2019. Signalp 5.0 improves signal peptide predictions using deep neural networks. Nat Biotechnol. 37:420–423. https://doi.org/10.1038/s41587-019-0036-z.

Amrine KCH *et al.* 2015. Comparative transcriptomics of Central Asian *Vitis vinifera* accessions reveals distinct defense strategies against powdery mildew. Hortic Res. 2:15037. https://doi.org/10.1038/hortres.2015.37.

Arnold CJ *et al.* 2024. Multiple routes to fungicide resistance: interaction of Cyp51 gene sequences, copy number and expression. Mol Plant Pathol. 25:e13498. https://doi.org/10.1111/mpp.13498.

Bankevich A *et al.* 2012. SPAdes: a new genome assembly algorithm and its applications to single-cell sequencing. J Comput Biol. 19:455–477. https://doi.org/10.1089/cmb.2012.0021.

Barrett K, Jensen K, Meyer AS, Frisvad JC, Lange L. 2020. Fungal secretome profile categorization of CAZymes by function and family corresponds to fungal phylogeny and taxonomy: example Aspergillus and Penicillium. Sci Rep. 10:5158. https://doi.org/10.1038/s41598-020-61907-1.

Behr M et al. 2012. Remodeling of cytokinin metabolism at infection sites of *Colletotrichum graminicola* on maize leaves. Mol Plant Microbe Interact. 25:1073–1082. https://doi.org/10.1094/MPMI-01-12-0012-R.

Beimforde C et al. 2014. Estimating the Phanerozoic history of the Ascomycota lineages: combining fossil and molecular data. Mol Phylogenet Evol. 78:386–398. https://doi.org/10.1016/j.ympev.2014.04.024.

Bettinelli P et al. 2023a. Towards marker-assisted breeding for black rot bunch resistance: identification of a major QTL in the grapevine cultivar "Merzling". Int J Mol Sci. 24:3568. https://doi.org/10.3390/ijms24043568.

Bettinelli P et al. 2023b. Breeding for black rot resistance in grapevine: advanced approaches for germplasm screening. Euphytica. 219:113. https://doi.org/10.1007/s10681-023-03235-9.

Blin K et al. 2021. antiSMASH 6.0: improving cluster detection and comparison capabilities. Nucleic Acids Res. 49:W29–W35. https://doi.org/10.1093/nar/gkab335.

Boetzer M, Pirovano W. 2014. SSPACE-LongRead: scaffolding bacterial draft genomes using long read sequence information. BMC Bioinformatics. 15:211. https://doi.org/10.1186/1471-2105-15-211.

Bolger AM, Lohse M, Usadel B. 2014. Trimmomatic: a flexible trimmer for illumina sequence data. Bioinformatics. 30:2114–2120. https://doi.org/10.1093/bioinformatics/btu170.

Bouckaert R et al. 2019. BEAST 2.5: an advanced software platform for Bayesian evolutionary analysis. PLoS Comput Biol. 15:e1006650. https://doi.org/10.1371/journal.pcbi.1006650.

Brakhage AA. 2013. Regulation of fungal secondary metabolism. Nat Rev Microbiol. 11:21–32. https://doi.org/10.1038/nrmicro2916.

Brown MR, Manuel Gonzalez de La Rosa P, Blaxter M. 2025. Tidk: a toolkit to rapidly identify telomeric repeats from genomic datasets. Bioinformatics. 41:btaf049. https://doi.org/10.1093/bioinformatics/btaf049.

Bruno VM et al. 2006. Control of the *C. albicans* cell wall damage response by transcriptional regulator Cas5. PLoS Pathog. 2:e21. https://doi.org/10.1371/journal.ppat.0020021.

Buijs VA, Zuijdgeest XCL, Groenewald JZ, Crous PW, de Vries RP. 2021. Carbon utilization and growth-inhibition of citrus-colonizing Phyllosticta species. Fungal Biol. 125:815–825. https://doi.org/10.1016/j.funbio.2021.05.003.

Cantu D, Massonnet M, Cochetel N. 2024. The wild side of grape genomics. Trends Genet. 40:601–612. https://doi.org/10.1016/j.tig.2024.04.014.

Cantu D, Vicente AR, Labavitch JM, Bennett AB, Powell ALT. 2008. Strangers in the matrix: plant cell walls and pathogen susceptibility. Trends Plant Sci. 13:610–617. https://doi.org/10.1016/j.tplants.2008.09.002.

Castresana J. 2000. Selection of conserved blocks from multiple alignments for their use in phylogenetic analysis. Mol Biol Evol. 17:540–552. https://doi.org/10.1093/oxfordjournals.molbev.a026334.

Chatterjee N, Shi J, García-Closas M. 2016. Developing and evaluating polygenic risk prediction models for stratified disease prevention. Nat Rev Genet. 17:392–406. https://doi.org/10.1038/nrg.2016.27.

Chen S et al. 2014a. Carbon cloth stimulates direct interspecies electron transfer in syntrophic co-cultures. Bioresour Technol. 173:82–86. https://doi.org/10.1016/j.biortech.2014.09.009.

Chen W et al. 2014b. Fungal cytochrome P450 monooxygenases: their distribution, structure, functions, family expansion, and evolutionary origin. Genome Biol Evol. 6:1620–1634. https://doi.org/10.1093/gbe/evu132.

Chen W, Jiang X, Yang Q. 2020. Glycoside hydrolase family 18 chitinases: the known and the unknown. Biotechnol Adv. 43:107553. https://doi.org/10.1016/j.biotechadv.2020.107553.

Cheng L-L, Thangaraj K, Deng C, Deng W-W, Zhang Z-Z. 2019. *Phyllosticta capitalensis* causes leaf spot on tea plant (*Camellia sinensis*) in China. Plant Dis. 103:2964. https://doi.org/10.1094/PDIS-04-19-0768-PDN.

Chin C-S et al. 2016. Phased diploid genome assembly with single-molecule real-time sequencing. Nat Methods. 13:1050–1054. https://doi.org/10.1038/nmeth.4035.

Choi J et al. 2014. fPoxDB: fungal peroxidase database for comparative genomics. BMC Microbiol. 14:117. https://doi.org/10.1186/1471-2180-14-117.

Cingolani P et al. 2012. A program for annotating and predicting the effects of single nucleotide polymorphisms, SnpEff. Fly (Austin). 6:80–92. https://doi.org/10.4161/fly.19695.

Colombo M et al. 2020. Nopv1: a synthetic antimicrobial peptide aptamer targeting the causal agents of grapevine downy mildew and potato late blight. Sci Rep. 10:17574. https://doi.org/10.1038/s41598-020-73027-x.

Črešnar B, Petrič Š. 2011. Cytochrome P450 enzymes in the fungal kingdom. Biochim Biophys Acta Proteins Proteomics. 1814:29–35. https://doi.org/10.1016/j.bbapap.2010.06.020.

Danecek P et al. 2021. Twelve years of SAMtools and BCFtools. Gigascience. 10:giab008. https://doi.org/10.1093/gigascience/giab008.

Darriba D et al. 2020. ModelTest-NG: a new and scalable tool for the selection of DNA and protein evolutionary models. Mol Biol Evol. 37:291–294. https://doi.org/10.1093/molbev/msz189.

Denny TP, Matthews PS, VanEtten HD. 1987. A possible mechanism of nondegradative tolerance of pisatin in *Nectria haematococca* MP VI. Physiol Mol Plant Pathol. 30:93–107. https://doi.org/10.1016/0885-5765(87)90085-3.

Denny TP, VanEtten HD. 1983. Tolerance of *Nectria haematococca* MP VI to the phytoalexin pisatin in the absence of detoxification. Microbiology. 129:2893–2901. https://doi.org/10.1099/00221287-129-9-2893.

De Silva N et al. 2016. Mycosphere essays 9: defining biotrophs and hemibiotrophs. Mycosphere. 7:545–559. https://doi.org/10.5943/mycosphere/7/5/2.

Drula E et al. 2022. The carbohydrate-active enzyme database: functions and literature. Nucleic Acids Res. 50:D571–D577. https://doi.org/10.1093/nar/gkab1045.

Durairaj P, Hur J-S, Yun H. 2016. Versatile biocatalysis of fungal cytochrome P450 monooxygenases. Microb Cell Fact. 15:125. https://doi.org/10.1186/s12934-016-0523-6.

Edgar RC. 2004. MUSCLE: multiple sequence alignment with high accuracy and high throughput. Nucleic Acids Res. 32:1792–1797. https://doi.org/10.1093/nar/gkh340.

Eichmeier A et al. 2022. Draft genome sequence of *Phyllosticta ampelicida*, the cause of grapevine black rot. Phytopathol Mediterr. 16:279–282. https://doi.org/10.36253/phyto-13516.

Finn RD et al. 2016. The Pfam protein families database: towards a more sustainable future. Nucleic Acids Res. 44:D279–D285. https://doi.org/10.1093/nar/gkv1344.

Fu H, Li W, Tang J. 2025. A cytochrome P450 AaCP1 is required for conidiation and pathogenicity in the tangerine pathotype of *Alternaria alternata*. Microorganisms. 13:343. https://doi.org/10.3390/microorganisms13020343.

Garcia JF et al. 2021. Phylogenomics of plant-associated Botryosphaeriaceae species. Front Microbiol. 12:652802. https://doi.org/10.3389/fmicb.2021.652802.

Garcia JF *et al.* 2024a. Genome analysis of the esca-associated Basidiomycetes *Fomitiporia mediterranea*, *Fomitiporia polymorpha*, *Inonotus vitis*, and *Tropicoporus texanus* reveals virulence factor repertoires characteristic of white-rot fungi. G3 (Bethesda). 14: jkae189. https://doi.org/10.1093/g3journal/jkae189.

Garcia JF *et al.* 2024b. Comparative pangenomic insights into the distinct evolution of virulence factors among grapevine trunk pathogens. Mol Plant Microbe Interact. 37:127–142. https://doi.org/10.1094/MPMI-09-23-0129-R.

Gilbert HJ, Knox JP, Boraston AB. 2013. Advances in understanding the molecular basis of plant cell wall polysaccharide recognition by carbohydrate-binding modules. Curr Opin Struct Biol. 23: 669–677. https://doi.org/10.1016/j.sbi.2013.05.005.

Glienke C *et al.* 2011. Endophytic and pathogenic Phyllosticta species, with reference to those associated with citrus black spot. Persoonia Mol Phylogeny Evol Fungi. 26:47–56. https://doi.org/10.3767/003158511X569169.

Guarnaccia V *et al.* 2019. *Phyllosticta citricarpa* and sister species of global importance to citrus. Mol Plant Pathol. 20:1619–1635. https://doi.org/10.1111/mpp.12861.

Han S *et al.* 2022. TIGER: technical variation elimination for metabolomics data using ensemble learning architecture. Brief Bioinform. 23:bbab535. https://doi.org/10.1093/bib/bbab535.

Hane JK, Paxman J, Jones DAB, Oliver RP, de Wit P. 2020. "CATAStrophy," a genome-informed trophic classification of filamentous plant pathogens—how many different types of filamentous plant pathogens are there? Front Microbiol. 10:492799. https://doi.org/10.3389/fmicb.2019.03088.

Haridas S *et al.* 2020. 101 Dothideomycetes genomes: a test case for predicting lifestyles and emergence of pathogens. Stud Mycol. 96:141–153. https://doi.org/10.1016/j.simyco.2020.01.003.

Hausmann L, Rex F, Töpfer R. 2017. Evaluation and genetic analysis of grapevine black rot resistances. Acta Hortic. 1188:285–290. https://doi.org/10.17660/ActaHortic.2017.1188.37.

Hoff KJ, Lange S, Lomsadze A, Borodovsky M, Stanke M. 2016. BRAKER1: unsupervised RNA-Seq-based genome annotation with GeneMark-ET and AUGUSTUS. Bioinformatics. 32:767–769. https://doi.org/10.1093/bioinformatics/btv661.

Horbach R, Navarro-Quesada AR, Knogge W, Deising HB. 2011. When and how to kill a plant cell: infection strategies of plant pathogenic fungi. J Plant Physiol. 168:51–62. https://doi.org/10.1016/j.jplph.2010.06.014.

Jack DL, Paulsen IT, Saier MH. 2000. The amino acid/polyamine/organocation (APC) superfamily of transporters specific for amino acids, polyamines and organocations. Microbiology. 146: 1797–1814. https://doi.org/10.1099/00221287-146-8-1797.

Jia M *et al.* 2023. Identification and analysis of the secretome of plant pathogenic fungi reveals lifestyle adaptation. Front Microbiol. 14: 1171618. https://doi.org/10.3389/fmicb.2023.1171618.

Jones L *et al.* 2014. Adaptive genomic structural variation in the grape powdery mildew pathogen, *Erysiphe necator*. BMC Genomics. 15: 1081. https://doi.org/10.1186/1471-2164-15-1081.

Keller NP. 2019. Fungal secondary metabolism: regulation, function and drug discovery. Nat Rev Microbiol. 17:167–180. https://doi.org/10.1038/s41579-018-0121-1.

Kim D, Paggi JM, Park C, Bennett C, Salzberg SL. 2019. Graph-based genome alignment and genotyping with HISAT2 and HISAT-genotype. Nat Biotechnol. 37:907–915. https://doi.org/10.1038/s41587-019-0201-4.

Kozlov AM, Darriba D, Flouri T, Morel B, Stamatakis A. 2019. RAxML-NG: a fast, scalable and user-friendly tool for maximum likelihood phylogenetic inference. Bioinformatics. 35:4453–4455. https://doi.org/10.1093/bioinformatics/btz305.

Krogh A, Larsson B, von Heijne G, Sonnhammer EL. 2001. Predicting transmembrane protein topology with a hidden Markov model: application to complete genomes. J Mol Biol. 305:567–580. https://doi.org/10.1006/jmbi.2000.4315.

Kubicek CP, Starr TL, Glass NL. 2014. Plant cell wall-degrading enzymes and their secretion in plant-pathogenic fungi. Annu Rev Phytopathol. 52:427–451. https://doi.org/10.1146/annurev-phyto-102313-045831.

Kuo K, Hoch HC. 1996a. Germination of *Phyllosticta ampelicida* pycnidiospores: prerequisite of adhesion to the substratum and the relationship of substratum wettability. Fungal Genet Biol. 20:18–29. https://doi.org/10.1006/fgbi.1996.0005.

Kuo K, Hoch HC. 1996b. The parasitic relationship between *Phyllosticta ampelicida* and *Vitis vinifera*. Mycologia. 88:626. https://doi.org/10.2307/3761158.

Li H *et al.* 2009. The sequence alignment/map format and SAMtools. Bioinformatics. 25:2078–2079. https://doi.org/10.1093/bioinformatics/btp352.

Li Z *et al.* 2025. Advances in the molecular mechanism of grapevine resistance to fungal diseases. Mol Hortic. 5:1. https://doi.org/10.1186/s43897-024-00119-x.

Li H, Durbin R. 2009. Fast and accurate short read alignment with Burrows–Wheeler transform. Bioinformatics. 25:1754–1760. https://doi.org/10.1093/bioinformatics/btp324.

Mair WJ *et al.* 2020. Parallel evolution of multiple mechanisms for demethylase inhibitor fungicide resistance in the barley pathogen *Pyrenophora teres* f. sp. maculata. Fungal Genet Biol. 145:103475. https://doi.org/10.1016/j.fgb.2020.103475.

Manni M, Berkeley MR, Seppey M, Simão FA, Zdobnov EM. 2021. BUSCO update: novel and streamlined workflows along with broader and deeper phylogenetic coverage for scoring of eukaryotic, prokaryotic, and viral genomes. Mol Biol Evol. 38:4647–4654. https://doi.org/10.1093/molbev/msab199.

Marín-Menguiano M, Moreno-Sánchez I, Barrales RR, Fernández-Álvarez A, Ibeas JI. 2019. N-glycosylation of the protein disulfide isomerase Pdi1 ensures full *Ustilago maydis* virulence. PLoS Pathog. 15:e1007687. https://doi.org/10.1371/journal.ppat.1007687.

McKenna A *et al.* 2010. The Genome Analysis Toolkit: a MapReduce framework for analyzing next-generation DNA sequencing data. Genome Res. 20:1297–1303. https://doi.org/10.1101/gr.107524.110.

Mendes FK, Vanderpool D, Fulton B, Hahn MW. 2021. CAFE 5 models variation in evolutionary rates among gene families. Bioinformatics. 36:5516–5518. https://doi.org/10.1093/bioinformatics/btaa1022.

Mingot JM, Peñalva MA, Fernández-Cañón JM. 1999. Disruption of phacA, an *Aspergillus nidulans* gene encoding a novel cytochrome P450 monooxygenase catalyzing phenylacetate 2-hydroxylation, results in penicillin overproduction. J Biol Chem. 274:14545–-14550. https://doi.org/10.1074/jbc.274.21.14545.

Minio A, Massonnet M, Figueroa-Balderas R, Castro A, Cantu D. 2019. Diploid genome assembly of the wine grape Carménère. G3 (Bethesda). 9:1331–1337. https://doi.org/10.1534/g3.119.400030.

Mir AA *et al.* 2015. Systematic characterization of the peroxidase gene family provides new insights into fungal pathogenicity in *Magnaporthe oryzae*. Sci Rep. 5:11831. https://doi.org/10.1038/srep11831.

Moktali V *et al.* 2012. Systematic and searchable classification of cytochrome P450 proteins encoded by fungal and oomycete genomes. BMC Genomics. 13:525. https://doi.org/10.1186/1471-2164-13-525.

Molitor D, Beyer M. 2014. Epidemiology, identification and disease management of grape black rot and potentially useful

metabolites of black rot pathogens for industrial applications—a review. Ann Appl Biol. 165:305–317. https://doi.org/10.1111/aab.12155.

Morales-Cruz A *et al.* 2015. Distinctive expansion of gene families associated with plant cell wall degradation, secondary metabolism, and nutrient uptake in the genomes of grapevine trunk pathogens. BMC Genomics. 16:469. https://doi.org/10.1186/s12864-015-1624-z.

Morales-Cruz A *et al.* 2020. Independent whole-genome duplications define the architecture of the genomes of the devastating West African cacao black pod pathogen *Phytophthora megakarya* and its close relative *Phytophthora palmivora*. G3 (Bethesda). 10: 2241–2255. https://doi.org/10.1534/g3.120.401014.

Moses V, Hatherley R, Tastan Bishop Ö. 2016. Bioinformatic characterization of type-specific sequence and structural features in auxiliary activity family 9 proteins. Biotechnol Biofuels. 9:239. https://doi.org/10.1186/s13068-016-0655-2.

Muellender MM, Mahlein A, Stammler G, Varrelmann M. 2021. Evidence for the association of target-site resistance in cyp51 with reduced DMI sensitivity in European *Cercospora beticola* field isolates. Pest Manag Sci. 77:1765–1774. https://doi.org/10.1002/ps.6197.

Nagesh P *et al.* 2023. Extending shared socio-economic pathways for pesticide use in Europe: pest-Agri-SSPs. J Environ Manage. 342: 118078. https://doi.org/10.1016/j.jenvman.2023.118078.

Nakayama N, Takemae A, Shoun H. 1996. Cytochrome P450foxy, a catalytically self-sufficient fatty acid hydroxylase of the fungus *Fusarium oxysporum*. J Biochem. 119:435–440. https://doi.org/10.1093/oxfordjournals.jbchem.a021260.

Navarre C. 2000. Membrane hyperpolarization and salt sensitivity induced by deletion of PMP3, a highly conserved small protein of yeast plasma membrane. EMBO J. 19:2515–2524. https://doi.org/10.1093/emboj/19.11.2515.

O'Brien JA, Daudi A, Butt VS, Paul Bolwell G. 2012. Reactive oxygen species and their role in plant defence and cell wall metabolism. Planta. 236:765–779. https://doi.org/10.1007/s00425-012-1696-9.

Ohm RA *et al.* 2012. Diverse lifestyles and strategies of plant pathogenesis encoded in the genomes of eighteen Dothideomycetes fungi. PLoS Pathog. 8:e1003037. https://doi.org/10.1371/journal.ppat.1003037.

Ortiz-Álvarez J *et al.* 2020. Phylogeny, evolution, and potential ecological relationship of cytochrome CYP52 enzymes in Saccharomycetales yeasts. Sci Rep. 10:10269. https://doi.org/10.1038/s41598-020-67200-5.

Ospina-Giraldo MD, Griffith JG, Laird EW, Mingora C. 2010. The CAZyome of *Phytophthora* spp.: a comprehensive analysis of the gene complement coding for carbohydrate-active enzymes in species of the genus Phytophthora. BMC Genomics. 11:525. https://doi.org/10.1186/1471-2164-11-525.

Paineau M, Zaccheo M, Massonnet M, Cantu D. 2025. Advances in grape and pathogen genomics toward durable grapevine disease resistance. J Exp Bot. 76: 3059–3070. https://doi.org/10.1093/jxb/erae450.

Pereira DA, McDonald BA, Brunner PC. 2017. Mutations in the CYP51 gene reduce DMI sensitivity in *Parastagonospora nodorum* populations in Europe and China. Pest Manag Sci. 73:1503–1510. https://doi.org/10.1002/ps.4486.

Pirrello C *et al.* 2019. Emergent Ascomycetes in viticulture: an interdisciplinary overview. Front Plant Sci. 10:1–30. https://doi.org/10.3389/fpls.2019.01394.

Précigout P-A, Claessen D, Makowski D, Robert C. 2020. Does the latent period of leaf fungal pathogens reflect their trophic type? A meta-analysis of biotrophs, hemibiotrophs, and necrotrophs. Phytopathology®. 110:345–361. https://doi.org/10.1094/PHYTO-04-19-0144-R.

Pryce-Jones E, Carver T, Gurr SJ. 1999. The roles of cellulase enzymes and mechanical force in host penetration by *Erysiphe graminis* f.sp. *hordei*. Physiol Mol Plant Pathol. 55:175–182. https://doi.org/10.1006/pmpp.1999.0222.

Rambaut A. 2018. Figtree, a graphical viewer of phylogenetic trees (Version 1.4.4). Institute of Evolutionary Biology, University of Edinburgh.

Reveglia P, Billones-Baaijens R, Savocchia S. 2022. Phytotoxic metabolites produced by fungi involved in grapevine trunk diseases: progress, challenges, and opportunities. Plants. 11:3382. https://doi.org/10.3390/plants11233382.

Rhie A *et al.* 2021. Towards complete and error-free genome assemblies of all vertebrate species. Nature. 592:737–746. https://doi.org/10.1038/s41586-021-03451-0.

Rinaldi PA *et al.* 2017. Genetic variability of *Phyllosticta ampelicida*, the agent of black rot disease of grapevine. Phytopathology®. 107: 1406–1416. https://doi.org/10.1094/PHYTO-11-16-0404-R.

Rodrigues CM, Takita MA, Silva NV, Ribeiro-Alves M, MacHado MA. 2019. Comparative genome analysis of *Phyllosticta citricarpa* and *Phyllosticta capitalensis*, two fungi species that share the same host. BMC Genomics. 20:1–12. https://doi.org/10.1186/s12864-019-5911-y.

Rosa S *et al.* 2023. The cyclic peptide G4CP2 enables the modulation of galactose metabolism in yeast by interfering with GAL4 transcriptional activity. Front Mol Biosci. 10:1017757. https://doi.org/10.3389/fmolb.2023.1017757.

Saier MH. 2000. A functional-phylogenetic classification system for transmembrane solute transporters. Microbiol Mol Biol Rev. 64: 354–411. https://doi.org/10.1128/MMBR.64.2.354-411.2000.

Saier MH *et al.* 2016. The Transporter Classification Database (TCDB): recent advances. Nucleic Acids Res. 44:D372–D379. https://doi.org/10.1093/nar/gkv1103.

Saier MH, Tran CV, Barabote RD. 2006. TCDB: the Transporter Classification Database for membrane transport protein analyses and information. Nucleic Acids Res. 34:D181–D186. https://doi.org/10.1093/nar/gkj001.

Santos RF, Ciampi-Guillardi M, Fraaije BA, de Oliveira AA, Amorim L. 2020. The climate-driven genetic diversity has a higher impact on the population structure of *Plasmopara viticola* than the production system or QoI fungicide sensitivity in subtropical Brazil. Front Microbiol. 11:575045. https://doi.org/10.3389/fmicb.2020.575045.

Silva M, Pereira OL, Braga IF, Lelis SM. 2008. Leaf and pseudobulb diseases on *Bifrenaria harrisoniae* (Orchidaceae) caused by *Phyllosticta capitalensis* in Brazil. Australas Plant Dis Notes. 3:53. https://doi.org/10.1071/DN08022.

Sirim D, Wagner F, Lisitsa A, Pleiss J. 2009. The Cytochrome P450 Engineering Database: integration of biochemical properties. BMC Biochem. 10:27. https://doi.org/10.1186/1471-2091-10-27.

Smit A, Hubley R, Green P. 2015a. RepeatMasker Open-4.1. 2013–2015. http://www.repeatmasker.org. Retrieved March 3, 2024.

Smit A, Hubley R, Green P. 2015b. RepeatModeler Open-1.0. 2008–2015. http://www.repeatmasker.org. Retrieved August 22, 2019.

Stanke M *et al.* 2006. AUGUSTUS: ab initio prediction of alternative transcripts. Nucleic Acids Res. 34:W435–W439. https://doi.org/10.1093/nar/gkl200.

Stukenbrock E, Gurr S. 2023. Address the growing urgency of fungal disease in crops. Nature. 617:31–34. https://doi.org/10.1038/d41586-023-01465-4.

Sui X-N, Guo M-J, Zhou H, Hou C-L. 2023. Four new species of Phyllosticta from China based on morphological and

phylogenetic characterization. Mycology. 14:190–203. https://doi.org/10.1080/21501203.2023.2225552.
Sützl L *et al.* 2018. Multiplicity of enzymatic functions in the CAZy AA3 family. Appl Microbiol Biotechnol. 102:2477–2492. https://doi.org/10.1007/s00253-018-8784-0.
Szabó M *et al.* 2023. Black rot of grapes (*Guignardia bidwellii*)—a comprehensive overview. Horticulturae. 9:130. https://doi.org/10.3390/horticulturae9020130.
Takemoto D, Scott B. 2023. NADPH oxidases in fungi. In: NADPH oxidases revisited: from function to structure. Cham: Springer International Publishing. p. 429–443. https://doi.org/10.1007/978-3-031-23752-2_25.
Timmer LW, Garnsey SM, Graham JH. 2000. Compendium of citrus diseases. St. Paul (MN): American Phytopathological Society.
Treangen TJ, Salzberg SL. 2012. Repetitive DNA and next-generation sequencing: computational challenges and solutions. Nat Rev Genet. 13:36–46. https://doi.org/10.1038/nrg3117.
Ullrich CI, Kleespies RG, Enders M, Koch E. 2009. Biology of the black rot pathogen, *Guignardia bidwellii*, its development in susceptible leaves of grapevine *Vitis vinifera*. J Für Kult. 61:82–90.https://doi.org/10.5073/JfK.2009.03.02.
Van Den Brink J, De Vries RP. 2011. Fungal enzyme sets for plant polysaccharide degradation. Appl Microbiol Biotechnol. 91:1477–1492. https://doi.org/10.1007/s00253-011-3473-2.
van Doorn WG *et al.* 2011. Morphological classification of plant cell deaths. Cell Death Differ. 18:1241–1246. https://doi.org/10.1038/cdd.2011.36.
van Ingen-Buijs VA *et al.* 2024. *Phyllosticta paracitricarpa* is synonymous with the EU quarantine fungus *P. citricarpa* based on phylogenomic analyses. Fungal Genet Biol. 175:103925. https://doi.org/10.1016/j.fgb.2024.103925.
Várnai A. *et al.* 2014. Carbohydrate-binding modules of fungal cellulases: occurrence in nature, function, and relevance in industrial biomass conversion. In: Sariaslani S, Gadd GM, editors. Advances in applied microbiology. Academic Press. p. 103–165. https://doi.org/10.1016/B978-0-12-800260-5.00004-8.
Vezzulli S, Doligez A, Bellin D. 2019. Molecular mapping of grapevine genes. In: Cantu D, Walker M, editors. The grape genome. Compendium of plant genomes. Cham: Springer. p. 103–136. https://doi.org/10.1007/978-3-030-18601-2_7.
Wang M *et al.* 2020. Genomic sequencing of *Phyllosticta citriasiana* provides insight into its conservation and diversification with two closely related Phyllosticta species associated with citrus. Front Microbiol. 10:2979. https://doi.org/10.3389/fmicb.2019.02979.
Wang C *et al.* 2021. Molecular characterization and overexpression of the difenoconazole resistance gene CYP51 in *Lasiodiplodia theobromae* field isolates. Sci Rep. 11:24299. https://doi.org/10.1038/s41598-021-03601-4.
Wikee S *et al.* 2013. *Phyllosticta capitalensis*, a widespread endophyte of plants. Fungal Divers. 60:91–105. https://doi.org/10.1007/s13225-013-0235-8.
Yang Y, Xiong D, Zhao D, Huang H, Tian C. 2024. Genome sequencing of *Elaeocarpus* spp. stem blight pathogen *Pseudocryphonectria elaeocarpicola* reveals potential adaptations to colonize woody bark. BMC Genomics. 25:714. https://doi.org/10.1186/s12864-024-10615-5.
Zhang C *et al.* 2020. Two point mutations on CYP51 combined with induced expression of the target gene appeared to mediate pyrisoxazole resistance in *Botrytis cinerea*. Front Microbiol. 11:1396. https://doi.org/10.3389/fmicb.2020.01396.
Zheng J *et al.* 2023. dbCAN3: automated carbohydrate-active enzyme and substrate annotation. Nucleic Acids Res. 51:W115–W121. https://doi.org/10.1093/nar/gkad328.

Editor: M. Sachs